



# Relative Effectiveness of a Radionuclide ( $^{210}\text{Pb}$ ), Surface Elevation Table (SET), and LiDAR At Monitoring Mangrove Forest Surface Elevation Change

Richard A. MacKenzie<sup>1</sup> · Ken W. Krauss<sup>2</sup> · Nicole Cormier<sup>3</sup> · Eugene Eperiam<sup>4</sup> · Jan van Aardt<sup>5</sup> · Ali Rouzbeh Kargar<sup>5</sup> · Jessica Grow<sup>6</sup> · J. Val Klump<sup>6</sup>

Received: 23 June 2023 / Revised: 1 November 2023 / Accepted: 2 November 2023  
© The Author(s) 2023

## Abstract

Sea-level rise (SLR) is one of the greatest future threats to mangrove forests. Mangroves have kept up with or paced past SLR by maintaining their forest floor elevation relative to sea level through root growth, sedimentation, and peat development. Monitoring surface elevation change (SEC) or accretion rates allows us to understand mangrove response to SLR and prioritizes resilient ecosystems for conservation or vulnerable ecosystems for restoration. We compared three methods to measure SEC and accretion in mangrove forests:  $^{210}\text{Pb}$ , surface elevation tables (SETs), and a terrestrial light detection and ranging system (compact biomass LiDAR—CBL). Lead-210 accretion rates were not significantly different than SET SEC rates and differences between the two methods ( $-2$  to  $2$  mm/year) were within the error of our measurements. Lead-210 only measures accretion in the upper meter of sediment and cannot capture deeper subsurface processes (e.g., subsidence, compaction) that SETs can. The lack of differences suggests the following: (1) surface processes in the active root zone are influencing forest floor elevation more than subsurface processes, (2) subsurface processes were not large enough to effect elevation, or (3) the SETs were not installed deep enough to capture subsurface processes. CBL SEC rates did not differ significantly from SET SEC rates. The larger spatial scale of the CBL scans resulted in significantly different SEC rates from some of the plots. This was due to the CBL measuring areas missed by the SET. The greater number of points measured by CBL ( $\sim 30,000$  vs  $36$ ) increased precision and lowered standard error. The traditional SET/rSET method is currently  $3\text{--}10\times$  cheaper than the  $^{210}\text{Pb}$  or CBL method, respectively, and can accurately track changes in forest floor elevation. Costs of the use of LiDAR are likely to decrease in the future with the advent of newer and more cost-effective technology.

**Keywords** Accretion · Resilience · Pacific · Mangroves · Active root zone · Subsurface processes

Communicated by Meagan Eagle

✉ Richard A. MacKenzie  
richard.mackenzie@usda.gov

- <sup>1</sup> USDA Forest Service, Pacific Southwest Research Station, Institute of Pacific Islands Forestry, Hilo, HI 96720, USA
- <sup>2</sup> U.S. Geological Survey, Wetland and Aquatic Research Center, 700 Cajundome Blvd., Lafayette, LA 70506, USA
- <sup>3</sup> Department of Earth and Environmental Sciences, Macquarie University, Sydney, NSW 2109, Australia
- <sup>4</sup> Pohnpei Forestry, Federated States of Micronesia, Kolonia, Pohnpei, USA
- <sup>5</sup> Chester F. Carlson Center for Imaging Science, Rochester Institute of Technology, Rochester, NY 14623, USA
- <sup>6</sup> University of Wisconsin at Milwaukee, School of Freshwater Sciences, 600 E. Greenfield Ave., Milwaukee, WI 53204, USA

## Introduction

Mangrove forests and the many ecosystem services they provide are threatened by predicted increased rates of sea-level rise (SLR). Over the past few centuries, many mangroves have kept up with SLR by maintaining the surface elevation of their forest floor relative to sea level through accretion (Alongi 2008; Rogers et al. 2019). Accretion is a process that involves root growth, sedimentation, resistance to soil compaction, and peat development (Krauss et al. 2014). The survival of today's mangroves is unclear as they face current or accelerated rates of SLR predicted to occur in the future. Will they be able to increase belowground productivity such that they can keep up with SLR? Will they respond to rising seas with shifts in their forest community structure creating novel ecosystems with better elevation

control? Furthermore, how will they respond to SLR in the presence of human activities that have increased over the last two centuries? For example, overharvesting of mangrove trees, conversion to other land uses, or roads and bridges that alter hydrological/sediment inputs or induce coastal squeeze negatively influence the natural response of mangroves to SLR (Kauffman et al. 2017; Krauss et al. 2010; Sharma et al. 2020; Woodroffe et al. 2015). All of these threats increase mangrove vulnerability to SLR. Monitoring surface elevation change (SEC) in mangroves can allow us to understand how they are responding to SLR, how various other anthropogenic stressors influence that response, and identify resilient ecosystems that can be prioritized for conservation or vulnerable ecosystems that may require some form of restoration.

Two methods are commonly used to track mangrove response to SLR around the world: surface elevation tables (SETs) (Webb et al. 2013) and naturally occurring

radionuclides (e.g.,  $^{210}\text{Pb}$ ,  $^{137}\text{Cs}$ ; Ranjan et al. 2011). The SET precisely measures mangrove forest floor elevation change over short periods of time (months to years) relative to the top of a series of permanently installed steel pipes (Table 1). Rods have replaced pipes over the last decade to provide better vertical stability (rSETs: Cahoon et al. 2002) (Fig. 1a). Measurements are made in four directions for a total of 36 readings (black circles in Fig. 1b). Because the pipes/rods are installed through the entire depth of the mangrove sediment, the SET/rSET is thought to have no bias in elevation change rates as it captures processes occurring throughout the depth of the mangrove soil (Table 1; Cahoon et al. 2002; Krauss et al. 2010). Traditional SET/rSET measurements rely on 36 points that require hours to measure and are prone to human error as pins need to be reset on the exact same point of the forest floor each time the SET/rSETs are read. Marker horizons (MH) are often deployed around SET/rSETs to track surface sedimentation

**Table 1** Comparison of the three methods used to measure accretion or surface elevation change. Initial cost reflects equipment (alpha detectors, SET arm, SET rods, CBL) needed to use technique in a plot. Costs do not include accessing the field plots or labor required to collect/process data. Once equipment has been purchased, the only costs

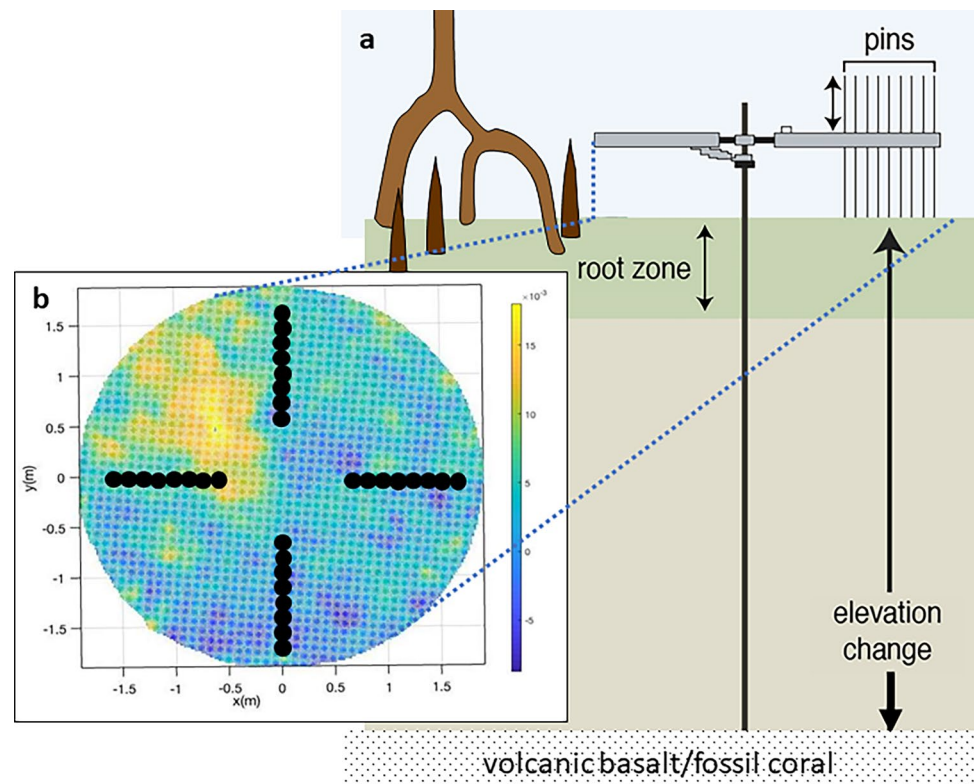
incurred for future measurements of plots/cores would be to access the field plots or for labor required to collect/process data. The  $^{210}\text{Pb}$  method would also require the costs of the chemicals (\$100). All costs are based off US prices (USD), which likely vary across regions or countries

Method	Pros	Cons	Initial cost for measurement of one plot/one core*
$^{210}\text{Pb}$	<ul style="list-style-type: none"> <li>- Long-term record that can measure accretion rates over the last century</li> <li>- Capable of determining rates at the sub-decadal scale</li> <li>- Only need to carry a corer into the mangrove to collect samples</li> </ul>	<ul style="list-style-type: none"> <li>- Measurement represents one point in the plot</li> <li>- Takes weeks to process cores</li> <li>- Influenced by biomixing</li> <li>- Cannot capture negative rates (shallow subsidence)</li> <li>- Short window to do field work as cores must be collected at low tide when there is no water on the forest floor</li> </ul>	<ul style="list-style-type: none"> <li>\$11,000 USD</li> <li>- Chemicals (\$100 USD)</li> <li>- 10 Alpha spectrometers (\$10,000 USD)</li> <li>- Sediment coring equipment (\$900 USD)</li> </ul>
SET/rSET	<ul style="list-style-type: none"> <li>- Captures belowground processes</li> <li>- Capable of measuring rates at a finer time scale resolution (months to years)</li> <li>- Measurements can be tied into a SLR datum for the most direct comparison between SEC and SLR</li> <li>- Longer window to do work as measurements can be taken when there is water on the forest floor</li> </ul>	<ul style="list-style-type: none"> <li>- Only measures 36 points</li> <li>- Human error in placing pins, need same person to read each year</li> <li>- Inconsistent surface references from earlier SET may complicate comparisons between sites</li> <li>- Measurement of plot can take hours</li> <li>- Requires carrying heavy equipment (generator, jack hammer, rods) into mangroves to install rods</li> </ul>	<ul style="list-style-type: none"> <li>\$5500 USD**</li> <li>- rSET arm (\$1500 USD)</li> <li>- rSET rods, receiver, driver (\$1500 USD)</li> <li>- Jack hammer (\$1000 USD)</li> <li>- Generator (\$1000 USD)</li> <li>- Misc. equip (\$500 USD)</li> </ul>
CBL	<ul style="list-style-type: none"> <li>- Scans 0.3 ha plot in minutes</li> <li>- High precision, low human error</li> <li>- Captures belowground processes</li> <li>- Capable of measuring rates at a finer time scale resolution (months to years)</li> <li>- Measurements can be tied into a SLR datum for the most direct comparison between SEC and SLR</li> </ul>	<ul style="list-style-type: none"> <li>- Large data sets to analyze</li> <li>- Inconsistent surface references from earlier SET may complicate comparisons between sites</li> <li>- Short window to do field work as cores must be collected at low tide when there is no water on the forest floor</li> <li>- Requires carrying heavy equipment (generator, jack hammer, rods) into mangroves to install rods</li> </ul>	<ul style="list-style-type: none"> <li>\$17,500 USD</li> <li>- rSET equipment (\$5500 USD)</li> <li>- CBL unit (\$12,000 USD)</li> </ul>

\*One core in this study was ten 2-cm intervals from 0 to 20 cm and ten 4-cm intervals from 20 to 60 cm

\*\* Assuming 20 1-m long stainless-steel rods are installed in the plot

**Fig. 1** Example of **a** SET/rSET system capturing elevation change throughout the entire depth profile of the mangrove and **b** the spatial resolution of a CBL scan (color) vs an SET (36 black symbols). For the CBL scan, warmer colors represent elevation gain and cooler colors represent elevation loss. There are several areas that were captured by the CBL but missed by the SET



or accretion rates (SAR). When these two measures are used together, subsurface change can be determined from SET/rSET measurements (Cahoon and Lynch 1997). MH have traditionally been feldspar, though other materials such as brick dust or sand have also been used. MH are typically deployed by sprinkling a 1-cm thick layer over  $50 \times 50$ -cm plots. A core is then taken and the sediment layer above the MH is measured (Callaway et al. 2013). While this has been an effective method used in salt marshes and mangroves along the east coast of the USA, it has not worked well in Pacific Island mangroves. Krauss et al. (2010) were not able to recover interpretable cores 9–15 months after deployment. This was due to biotic activity (e.g., sesarmid crabs, mudskippers) dispersing the feldspar layer. As a result, feldspar had to continually be deployed until it was eventually abandoned (Krauss et al. 2010). Newer methods using window screen have developed and seem like a promising alternative, especially in the presence of biotic activity (Swales and Lovelock 2020).

Lead-210 measures accretion, or the thickness/height of material added to the soil column above a given reference point (e.g., Robbins and Edgington 1975; Smoak et al. 2013). Lead-210 is a decay (daughter) product of the Uranium-238 ( $^{238}\text{U}$ ) series. Radon-222 ( $^{222}\text{Rn}$ ) gas produced from  $^{238}\text{U}$  in the earth's core degasses to the atmosphere. Here, it radioactively decays to  $^{210}\text{Pb}$ , which attaches to particles in the atmosphere that are deposited onto the earth's surface at a

constant rate through precipitation events (Robbins 1978). Sedimentation in coastal ecosystems results in the deposition of externally produced or “excess”  $^{210}\text{Pb}$  onto the sediment surface that starts to decay radioactively once buried and is no longer replenished from the atmosphere (Fig. 2). Using the laws of radioactivity decay and either the constant rate of supply (CRS) method (Appleby and Oldfield 1978) or the rapid steady-state mixing model (RSSM) (Robbins 1975), sediment cores can be dated up to 100 years using  $^{210}\text{Pb}$ . Accretion rates (mm/year) are then determined by dividing the soil depth intervals by their age. Excess  $^{210}\text{Pb}$  is rarely present below 1 m of soil and cannot be used to capture subsurface processes occurring below the core depth. Cores are expensive to analyze ( $\sim \$1000$  USD/core) and require several weeks to process (Table 1).

A terrestrial light detection and ranging system (compact biomass LiDAR—CBL) serves as a third novel method to measure SEC. To the best of our knowledge, CBL has rarely been used in this application (Rouzbeh Kargar et al. 2020) and offers a broader sampling capacity, greater precision, and lower error. A modified SET/rSET arm was developed to attach a CBL scanner to the top of the SET/rSET described above. The CBL rotates horizontally  $180^\circ$  to provide a  $270 \times 360^\circ$  scan of the entire radius forest plot, which can be up to 3 m in radius. Each scan samples 30,000–100,000 points (Fig. 1b) from the entire forest plot in minutes. Surface elevation change can then be

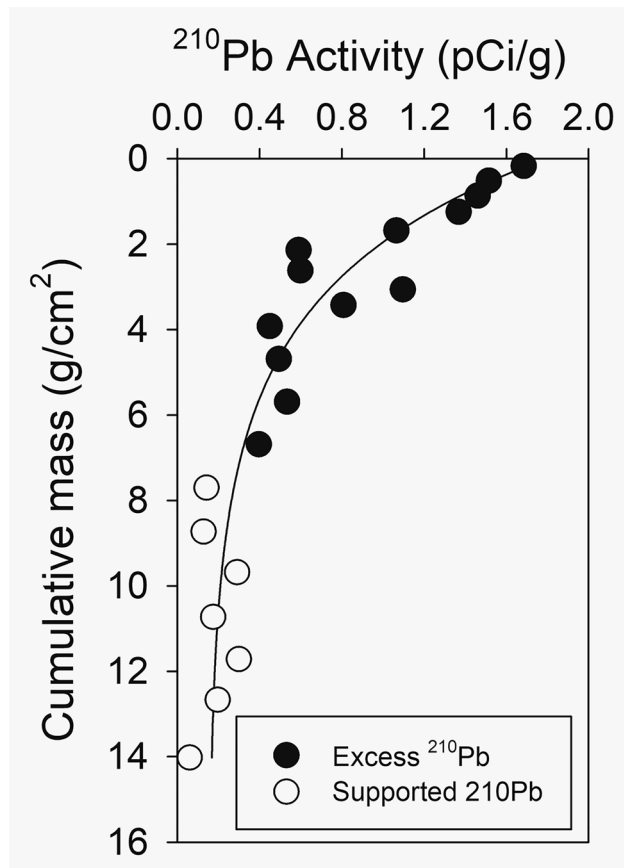


**Fig. 2** Example of a  $^{210}\text{Pb}$  profile measured in a sediment core against cumulative mass (MacKenzie et al. 2016). The solid symbols represent externally produced and delivered excess  $^{210}\text{Pb}$ , while the hollow circles represent in situ produced supported  $^{210}\text{Pb}$

measured by comparing the elevations of each point over time (e.g., every 6 months, every year). Because the CBL uses a laser to make measurements, there is low human error. The CBL is also attached to the SET/rSET that has been installed throughout the mangrove soil profile and is thought to have no bias in elevation change rates and can capture belowground processes. The only major drawback aside from the initial cost of the CBL unit is that the CBL generates enormous data sets that require several weeks to process (Table 1).

Studies using either the SET/rSET or  $^{210}\text{Pb}$  methods have yielded different results. Accretion rates of mangrove forests determined from radionuclides (e.g.,  $^{210}\text{Pb}$ ,  $^{137}\text{Cs}$ ) suggest that most mangroves are keeping up with current rates of sea-level rise (Fig. 3; Alongi 2008; Breithaupt et al. 2018; MacKenzie et al. 2016), while SEC of mangroves determined from SETs suggests otherwise. Lovelock et al. (2015b) reported that nearly 70% of the mangroves monitored with SETs are not keeping up with current SLR rates. Despite the different outcomes of the SET versus  $^{210}\text{Pb}$  studies, few attempts have been made to compare these methods

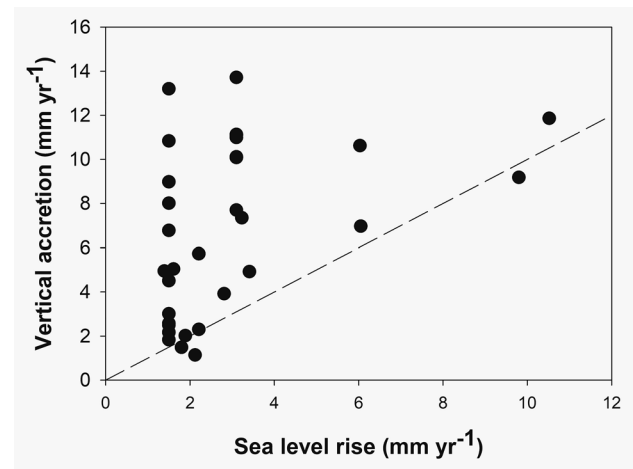


**Fig. 3** Comparison of accretion rate and RSLR. The dashed line represents a 1:1 line where both measures agree. The majority of the accretion rates are above this line suggesting these mangrove forest plots are keeping up with RSLR. Data from Alongi (2008) and MacKenzie et al. (2016)

side by side to determine potential differences in precision and accuracies and thus their ability to quantify mangrove response to SLR.

Monitoring mangrove response to SLR is a global issue. Mangroves that are keeping up with SLR and are considered resilient could be prioritized for conservation. Mangroves not keeping up with SLR and being considered vulnerable may require more active management or restoration efforts. But what is the best method to monitor these mangroves? Micronesia mangroves were used as model systems to examine this due to their temporally and spatial compact size and the long-term data sets available from them (Lovelock et al. 2015a). Results are likely applicable to other mangroves around the world.

The main objective of this study was to do side-by-side comparisons of three different methods to determine their accuracy of measuring accretion and surface elevation change in mangroves. Results could help identify the most suitable and cost-effective method that could be used for future mangrove monitoring efforts. Specifically,  $^{210}\text{Pb}$  accretion rates were compared to SET SEC rates from the same 17 permanent mangrove monitoring plots on the island of Pohnpei in the Federated States of Micronesia to examine how these two methods might differ in monitoring mangrove response to SLR. Comparisons between  $^{210}\text{Pb}$  accretion rates and MH SAR were not possible due to a lack of MH SAR data from the sites (Krauss et al. 2010) coupled with the differences in temporal scales captured by the two processes (i.e., decades to years, respectively). CBL SEC rates were also compared to SET SEC rates in eight of those plots to examine how these two methods might also differ in monitoring mangrove response to SLR.

## Methods

### Study Location

Triplicate forest plots were established in the fringe, riverine, and interior zone of the Enipoas and Sapwalap mangroves on the high island of Pohnpei in September 1998 (Krauss et al. 2010). Pohnpei (6° 51' N; 158° 19') is one of the four states of the Federated States of Micronesia located in the western Pacific and is a dormant volcanic island that is the tallest (790 m) and largest island (334 km<sup>2</sup>) in the Federated States of Micronesia. The island receives 4775 mm of rainfall annually in coastal areas and up to 7600 mm of rainfall in its mountains that feeds several rivers/streams. The mean annual temperature is 31.9° (Lander and Khosrowpanah 2004). Mangrove forests covered 6426 hectares of the island in 2018 (Woltz et al. 2022) representing nearly 20% of the total land area. There are eleven species of true mangrove trees found there that include the following: *Bruguiera gymnorrhiza*, *Heritiera littoralis*, *Lumnitzera littorea*, *Nypa fruticans*, *Pemphis acidula*, *Rhizophora apiculata*, *R. x lamarckii*, *R. mucronata*, *R. stylosa*, *Sonneratia alba*, and *Xylocarpus granatum* (Duke 1999).

### Surface Elevation Tables

Aluminum pipes (7.6 cm in diameter) were driven into the soil as far as possible using a manual slammer and backfilled with cement. A notched insert tube was attached to the top of each pipe. A portable SET arm was then attached to the insert tube on each pipe during each measurement period, where nine brass or fiberglass rods were lowered through holes into the arm until they rested on the mangrove surface. Measurements were made in four separate directions per SET pipe for a total of 36 measurements made during each measurement period. Measurements occurred bi-annually through 2000 and then annually from 2002 to 2004 and from 2015 to 2019 (Krauss et al. 2010; Lovelock et al. 2015b).

### Lead-210

A single 1-m-long sediment core was collected from each plot in 2016 using an open-faced gouge auger and sectioned into continuous 2-cm intervals from 0 to 20 cm and 4-cm intervals from 20 to 60 cm. Sediment cores were typically collected 1–2 m from the SET plots. Sediment intervals were returned to the lab, dried to a constant mass at 60 °C, and weighed to the nearest 0.1 g. Sediment samples (including fine roots) were ground into a fine powder using a mortar and pestle and a Wiley™ mill and then sieved through a 2-mm mesh sieve to remove any large roots or shells. Lead-210

activity was determined by measuring its decay product, Polonium-210 (<sup>210</sup>Po). Polonium-210 was extracted from ground sediment samples using hot acid digestion, plated onto copper discs, and then measured using alpha spectrometry at the University of Wisconsin-Milwaukee School of Freshwater Sciences (MacKenzie et al. 2016). We chose this method over direct counts of <sup>210</sup>Pb using gamma spectrometry because alpha spectrometry of <sup>210</sup>Po (1) requires less sediment (<0.5 g) than gamma counting (~10 g), (2) captures a better detection limit as <sup>210</sup>Pb is a weak alpha emitter (below the 46.52 keV limit of alpha detectors) and activities were generally low in our cores, and (3) requires less time to read 100's of samples (MacKenzie et al. 2016; Ranjan et al. 2011). Average activity of supported <sup>210</sup>Pb produced from within sediments was determined by plotting total <sup>210</sup>Pb activity versus depth and fitting a radioactive decay curve to the data in Sigma Plot v14.0 (Systat Software Inc., San Jose, CA). Average activity of supported <sup>210</sup>Pb was then determined by averaging the values along the asymptote. Excess <sup>210</sup>Pb was calculated for each interval by subtracting the average supported <sup>210</sup>Pb activity from the total <sup>210</sup>Pb activity. Each interval was then dated using the CRS method (Appleby and Oldfield 1978) and accretion rates (cm year<sup>-1</sup>) were determined by dividing the depth interval (cm) by the number of years of that interval.

### Compact Biomass LiDAR (CBL)

The surface elevation was scanned in the Enipoas ( $n = 1$ ) and Sapwalap ( $n = 7$ ) forest plots at low tide in 2017 and 2019, using a low-cost, rapid-scan terrestrial laser scanner (CBL; SICK LMS-151, SICK AG Waldkirch, Germany). The CBL used a 905-nm laser pulsing at 27 kHz and collected data across a 270° × 360° zenith × azimuth “hemisphere” (the 90° cone above the scanner remains unscanned). A brief overview of the approach is provided here; interested readers are referred to Rouzbeh-Kargar et al. (2020) for a more detailed description.

The scans were co-registered using a combination of manual and automatic approaches, by using structural tie points between the LiDAR point clouds, via a pairwise registration technique (Zai et al. 2017). The Iterative Closest Point (ICP) algorithm was then used to align the point clouds more accurately (Besl and McKay 1992). The resulting point clouds were aligned with those from 2017, after registering all the plot scans for 2019 data, in order to avoid any spatial and angular displacement between the collected ground points. Point clouds were also downsampled since the areas closest to the scanner and directly at its nadir (0° zenith) were highly oversampled due to the oversampling bias of the scanner in these regions. The downsampling algorithm was based on the spherical sampling scheme of the CBL and considered higher weights for the points further from the scanner, while assigning lower weights to points in

closer proximity (Fafard et al. 2020). Noise points in the data (i.e., outliers that do not relate to any structure in the LiDAR point cloud) were then removed using the Statistical Outlier Removal (SOR) algorithm (Rusu et al. 2008).

Next, the points in the LiDAR point cloud were classified into ground and non-ground returns in order to generate plot-level digital elevation models (DEMs) using the CSF algorithm (Zhang et al. 2016). This algorithm yielded the first output for refinement to accurately detect ground LiDAR returns. However, conventional ground detection algorithms may not yield very accurate ground returns, mainly due to the structural complexity and increased shadowing (occlusion) effects in CBL data. Root points were therefore visually identified that were classified as ground, while also filtering the detected ground returns based on their angular orientation in order to remove these erroneous points (Dewez et al. 2016).

The DEM interpolation was constrained to areas within each scanned plot that had adequate CBL point densities and did not include areas that had low point returns or highly variable LiDAR point densities. The resulting radii of interpolation ranged between 1.8 and 3.1 m among the various plots. The kriging interpolation technique (Trochu 1993) was used to interpolate ground returns to a  $1 \times 1$  cm ( $x, y$ ) grid resolution. A linear Nearest Neighbor Search (NNS) technique next was applied to the 2D grid of  $x$  and  $y$  coordinates from the two DEMs (Zlot and Bosse 2009) in order to compare the exact same points from 2017 and 2019 data. Finally, the elevation ( $Z$  values) of the corresponding points of the two DEMs was subtracted to identify locations where either an elevation gain or loss had occurred between 2017 and 2019 and its associated value. Extreme points (e.g., foot prints, fallen logs) were removed based on observations of the field crew or examination of plot photos. The average of the elevation change in each plot was then determined, and the consistency was assessed by comparing the LiDAR-derived SEC with the field-measured elevation data collected by SETs.

## Statistical Analysis

Both accretion and surface elevation change (SEC) rates were calculated using the following methods. For SET data, cumulative surface elevation measurements were plotted over time and then linear regression analyses were used to predict SEC rates based on the slope of the line. For  $^{210}\text{Pb}$ , we chose depth intervals that spanned the same time period as the SET data (e.g., 1999–2017). Cumulative depth measurements (i.e., 0, 20, 40, 60 mm) were then plotted against the age of that interval determined using  $^{210}\text{Pb}$  and the CRS method. Linear regression analyses were then used to predict accretion rates based on the slope of the line. All linear

regression analyses were conducted using Sigma Plot 14 (Systat Software, Inc., San Jose, CA).

Lead-210 accretion rates and SET SEC rates were compared using the Bland and Altman Statistical method of testing for agreement of clinical methods (Bland and Altman 1986, 1999). This method is a graphical representation used to evaluate agreement between two tests. Interpretation depends on the predetermined conditions and requirements. Differences between  $^{210}\text{Pb}$  accretion and SET SEC were plotted against the average of the rates from the two methods. Plotting against the average value vs plotting against either separate value avoids statistical artifacts that can be generated using the latter approach. The limits of agreements were equal to the upper and lower 95% confidence intervals. Mean values (bias) and the upper and lower limits of agreement were calculated using the SimplyAgree package (Caldwell 2022) in R (R Core Team 2013).

Both methods were also compared using a mixed effects log-normal model that controlled for site, mangrove, and subject effects in the glmmTMB package (Brooks et al. 2017) in R (R Core Team 2013). We used a likelihood ratio test to compare models with and without a method effect. If the method effect was not significant, then the null hypothesis that these methods were providing equivalent measurements on average was not rejected, controlling for the other effects.

SEC rates were also compared between SET and the CBL measurements made in the eight plots described above in 2017 and 2019. For SETs, SEC was calculated as the cumulative change in elevation from 2017 and 2019. SEC rates were then compared using the same methods used to compare  $^{210}\text{Pb}$  and SET above.

All variances reported are standard error (SE).

## Results

### Lead-210 vs SET

Accretion rates from  $^{210}\text{Pb}$  were all positive values, ranged from 0.51 to 6.6 mm/year, and had goodness of fits ( $R^2$ ) greater than 0.9 (Fig. 4; Table 2). The high  $R^2$  values were attributed to there often only being 3 depth intervals that occurred over the same time span as the SET measurements. SET SEC rates ranged from  $-0.74$  to 5.45 mm/year, had several negative measurements, and had goodness of fits that were above 0.6, although Sapwalap Fringe had poor  $R^2$  values of 0.30 and 0.05.

There were no significant differences between average  $^{210}\text{Pb}$  accretion rates ( $2.78 \pm 1.48$  mm/year) and SET SEC rates ( $2.59 \pm 1.81$  mm/year;  $X^2(1, 16) = 0.43$ ,  $p = 0.51$ ; Fig. 5a). Disparity between  $^{210}\text{Pb}$  accretion rates and SET SEC rates was on average  $0.2 \pm 1.7$  mm/year (Fig. 5b). Scattering of values around the mean suggests there is no bias

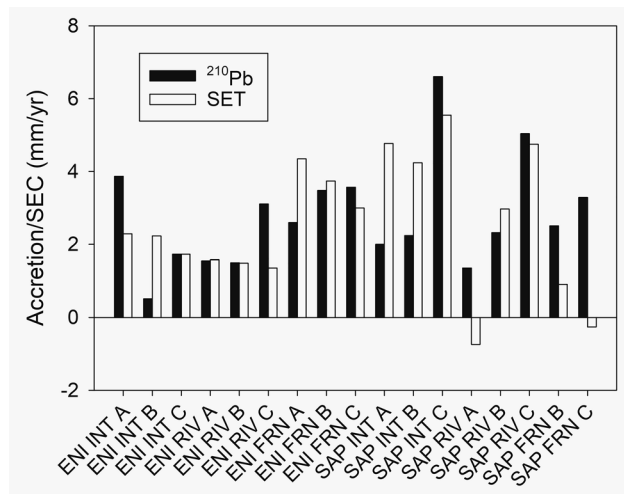


**Fig. 4** Comparison of accretion and surface elevation rates (mm/year) measured by <sup>210</sup>Pb (black) and SETs (white), respectively. Rates were measured through linear regressions (see “Methods” section) and therefore variance could not be calculated

(Fig. 5b); <sup>210</sup>Pb does not always over or under predict accretion rates compared to SET SEC rates. The majority of plots (15) fell within the calculated levels of agreement, where <sup>210</sup>Pb accretion rates ranged from being 1.90 mm/year below to 2.32 mm/year above the SET SEC measurements and are within the standard deviation of the differences. This

**Table 2** Lead-210 (<sup>210</sup>Pb) accretion (acc.) rates, SET surface elevation change (SEC) rates, and the difference (diff.) between the two measurements. The goodness of fit (*R*<sup>2</sup>) for both calculations is also reported to the right of each calculation

Plot	<sup>210</sup> Pb Acc. (mm/yr)	<i>R</i> <sup>2</sup> ( <sup>210</sup> Pb)	SET SEC (mm/yr)	<i>R</i> <sup>2</sup> (SET)	Diff
ENI INT A	3.87	0.99	2.29	0.84	1.58
ENI INT B	0.51	0.99	2.23	0.85	-1.72
ENI INT C	1.73	1.00	1.73	0.73	0.00
ENI RIV A	1.55	1.00	1.58	0.84	-0.03
ENI RIV B	1.50	0.98	1.49	0.68	0.01
ENI RIV C	3.11	0.99	1.36	0.65	1.75
ENI FRN A	2.60	0.99	4.35	0.95	-1.76
ENI FRN B	3.48	0.99	3.74	0.90	-0.26
ENI FRN C	3.57	0.99	3.00	0.92	0.56
SAP INT A	2.00	0.98	4.77	0.96	-2.77
SAP INT B	2.24	0.98	4.24	0.90	-2.00
SAP INT C	6.61	0.95	5.55	0.96	1.06
SAP RIV A	1.36	0.91	-0.74	0.39	2.10
SAP RIV B	2.32	0.89	2.97	0.87	-0.65
SAP RIV C	5.04	0.92	4.75	0.92	0.29
SAP FRN B	2.51	1.00	0.91	0.31	1.60
SAP FRN C	3.29	0.87	-0.26	0.05	3.55

suggests that these two methods are in agreement with each other and could potentially be used interchangeably.

**CBL vs SET**

CBL SEC rates ranged from -6.9 to 6.0 mm/year, while SET SEC rates ranged from -6.0 to 7.28 mm/year (Fig. 6; Table 3). Standard deviation from CBL measurements was an order of magnitude lower than SET measurements.

There were no significant differences between the average CBL SEC rate (-0.065 ± 4.32 mm/year) and SETs (0.53 ± 4.95 mm/year; X<sup>2</sup>(1, 7) = 0.75, *p* = 0.39; Fig. 7a). CBL SEC rates were on average 0.6 ± 2.0 mm/year below SET SEC rates, with 6 of the 8 plots falling within the confidence limits of the bias (Fig. 7b). While there are fewer points to compare than the <sup>210</sup>Pb vs SET, the majority of plots had differences that were less than zero, suggesting that CBL SEC rates were generally lower than SET SEC rates. Most plots (7) fell within the calculated levels of agreement, where CBL SEC rates ranged from being 3.2 mm/year below to 2.0 mm/year above the SET measurements. Again, most of the differences are within the standard deviation of the average differences, which suggests that these two methods are in agreement with each other and could potentially be used interchangeably.

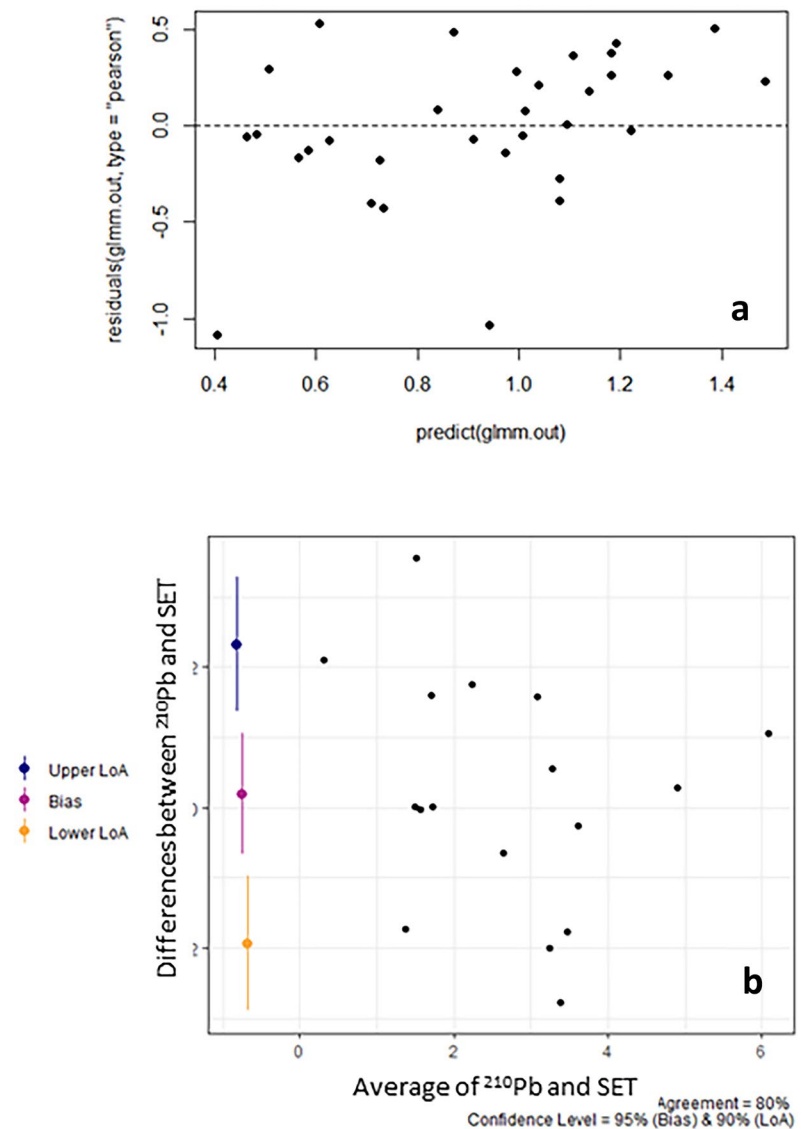
**Discussion**

**<sup>210</sup>Pb vs SET**

We found no differences between <sup>210</sup>Pb accretion rates and SET SEC rates calculated over the same time period (1999–2017). Most sites had disparate readings of only 2 to -2 mm/year. While these differences may make a difference when compared to the RSLR Pohnpei has experienced over this same time period (3.75 mm/year, Holgate et al. 2013; PSMFS 2023), they were within the error of our measurements as well as the level of acceptance defined by Bland and Altman (1986). There was no consistent difference between the measurements, which suggests they are both tracking similar mangrove responses to SLR. It is not clear if one method is better than the other at capturing mangrove forest floor response, only that more sediment cores or SETs/rSETs per plot will increase the precision and accuracy of the measurements.

Other studies have also reported no differences between <sup>210</sup>Pb and SET measurements. Given that decadal surface accretion rates (SAR) were derived from SETs and centennial SAR from <sup>210</sup>Pb, Breithaupt et al. (2018) report differences of 0–2.5 mm/year. Average decadal and centennial SAR were not statistically different (*p* > 0.05). Similarly, sediment accumulation rates measured using SET and <sup>210</sup>Pb

**Fig. 5** Scatterplot of **a** residuals from the GLMM test comparing  $^{210}\text{Pb}$  accretion rates to SET SEC rates and **b** agreement showing the bias and upper and lower level of agreements based on the Bland and Altman test (1986)



in New Zealand and Australia were not different (Rogers et al. 2014; Swales et al. 2015). Mean mangrove sediment accumulation rates varied by only 0.5–1.0 mm between  $^{210}\text{Pb}$  and SET measurements. Cahoon and Lynch (1997) used both marker horizons and  $^{210}\text{Pb}$  to track accretion and SETs to measure elevation. Marker horizons and  $^{210}\text{Pb}$  accretion rates differed by 3–7 mm, while  $^{210}\text{Pb}$  accretion and SET elevation generally differed by a few mm. Alternatively, Parkinson et al. (2017) reported a much larger difference between  $^{210}\text{Pb}$  and SET measurements from Gulf of Maine and Gulf of Mexico salt marshes (~12 mm) and Gulf of Mexico mangroves (4 mm). However, it is not clear if these were side-by-side comparisons within the same plots or comparisons of data from across the same regions.

The naturally occurring radionuclide  $^{210}\text{Pb}$  and SET/rSETs are often described as measuring two different processes: accretion and surface elevation change, respectively.

While both are reported as mm/year or cm/year, accretion/surface accretion is defined as the thickness or height of material added to the soil column above a given reference plane. Surface elevation change is the change in wetland surface height relative to a vertical horizontal reference plane. For early (pipe) SETs, the original measurement was the reference, while more recent installments/measurements have standardized the starting elevation to a vertical datum (Cahoon et al. 2002). Surface elevation includes both accretion and subsurface processes such as decomposition, mechanical compaction, and subsidence (Cahoon et al. 2002). Given that these two methods are often attributed to measuring two different metrics, when compared side by side in this and other studies, they produce results that only differ by a few mms and that are within the error of the measurements. This suggests that either subsurface processes such as subsidence or compaction were having



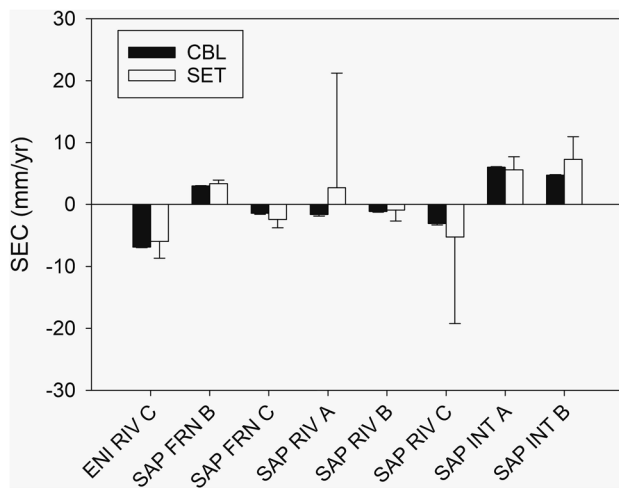


**Fig. 6** Comparison of average ( $\pm 1$  SE) surface elevation rates (mm/year) measured by Compact Biomass LiDAR (CBL; black) and SETs (white), respectively

a minimal impact on the measurements made in these sites (but see Saintilan et al. 2020), the original SET pipes were not installed deep enough to capture subsurface properties, or surface processes in the active root zone were important enough drivers to maintain surface elevation in these systems (e.g., Krauss et al. 2014; Osland et al. 2012). A study conducted in Pohnpei found that organic matter accumulation from root growth was the most important factor driving accretion rates (MacKenzie et al. in review). Similar results were reported from Belize mangroves (McKee et al. 2007). In Florida, soil elevation change in a mangrove after Hurricane Wilma was attributed to expansion of the active root zone (Whelan et al. 2009). While one could argue that these phenomena are only relevant to the handful of studies discussed above, it has been reported from several sites and

**Table 3** Average SEC rates ( $\pm 1$  SE) for the compact biomass LiDAR (CBL) and surface elevation table (SET) measurements for each plot where measurements were made. Species represent the percent contribution of each mangrove species to that forest plot measured and include *Bruguiera gymnorrhiza* (BRGY) and *Rhizophora* species (RHSP) that are comprised of *R. apiculata*, *R. mucronata*, and *R. stylosa*

Plot	Species	CBL SEC (mm/yr)	SET SEC (mm/yr)
	BRGY (64%)		
ENI RIV C	RHSP (33%)	-6.92 (0.08)	-6 (2.64)
SAP FRN B	RHSP (60%)	2.97 (0.06)	3.36 (0.57)
SAP FRN C	RHSP (60%)	-1.44 (0.15)	-2.45 (1.33)
SAP RIV A	RHSP (67%)	-1.62 (0.25)	2.68 (18.55)
SAP RIV B	RHSP (67%)	-1.14 (0.10)	-0.9 (1.78)
SAP RIV C	RHSP (67%)	-3.1 (0.22)	-5.29 (13.94)
SAP INT A	RHSP (60%)	6.01 (0.08)	5.59 (2.11)
SAP INT B	RHSP (60%)	4.72 (0.10)	7.28 (3.66)

from different types of mangroves. Clearly, more studies are needed to examine this.

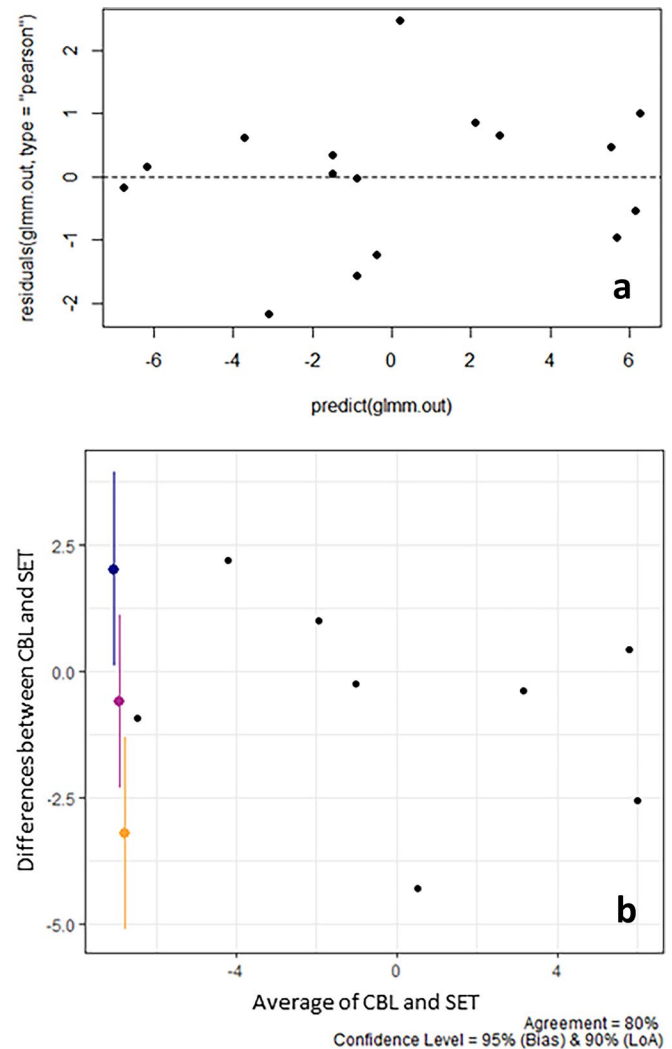
### CBL vs SET

CBL SEC rates were typically within 1 mm (0.2–1.1 mm) of the SET measurements made between 2015 and 2017. The only exceptions were Sapwalap Riverine A (4.3 mm) and C (2.2 mm) and Sapwalap Interior B (2.6 mm). This was due to elevation changes captured in the larger area scanned by the CBL that were out of the range and missed by the traditional 36 SET pin measurements (i.e., Fig. 1b). Standard error from CBL SEC measurement was also 10–70 $\times$  lower than SET SEC measurements.

The CBL method significantly decreases the labor and time requirements in the field to measure SEC data compared to more traditional SETs/rSETs (minutes versus hours) used around the world (Webb et al. 2013). Moreover, CBL increases SEC measurement accuracy by measuring a greater number of points within the forest plots and reduces human error associated with the replacement of SET pins during re-measurements. For example, the SET method uses 36 points per plot for SEC measurement, all of which are assessed by lowering the pins down until they are resting on the forest floor surface. This approach introduces some bias and error when the operator deems the SET pins have made full contact with the underlying surface or if the operator pushes the pins into the sediment. Measurements where a SET pin is placed on the sediment surface in one year but that is placed on debris, sticks, or crab burrows that appear the next year may have to be thrown out. This reduces the accuracy of SET measurements that rely on 36 points to assess the entire plot around the SET that is captured by the CBL (Kargar et al. 2020). The CBL-based approach, on the other hand, is completely automated (unbiased) in its 3D scanning operation and yields upwards of 30,000 elevation points per plot. This increases the repeatability and reliability of the CBL method compared to more traditional SET pin measurements. This also results in significantly lower error (Table 3).

The use of CBL for SEC measurements significantly expands localized SET plot measurements to a larger plot-level scan radius (e.g., 1.8 to 3.1 m, only restricted by the LiDAR scanner engineering specifications). The larger area allows the CBL to capture changes in elevation that the SET pins can miss. This is evidenced by the large differences observed between SEC measurements made in the Sapwalap Riverine A, Riverine C, and Interior C sites (Table 3). Another benefit of the CBL method over the SET method is that the scans can also be used to measure forest biomass, including complex root structures such as *Rhizophora* sp. prop roots that are not always included in traditional allometric methods (Kargar et al. 2020).

**Fig. 7** Scatterplot of **a** residuals from the GLMM test comparing CBL to SET SEC rates and **b** agreement showing the bias and upper and lower level of agreements based on the Bland and Altman test (1986)



Although potentially more efficient, there are drawbacks using the CBL method to assess mangrove forest SEC. The main drawback is that CBL measurements can only be performed when the forest floor is exposed (e.g., low tide, after significant rainfall events), since the 905-nm laser of the CBL used in this work cannot penetrate the water, and as a result, the submerged ground surface cannot be detected. Future efforts could be improved by using LiDAR systems in which the laser wavelength range can penetrate water. Furthermore, complex root structure can inhibit the ground detection accuracy of the CBL sensor. Plots that had higher *Rhizophora* sp. densities typically had more complex prop root structures that resulted in higher standard errors (Table 3) and decreased consistencies when CBL SEC was compared to SET SEC rates (see Rouzbeh Kargar et al. 2020).

The CBL approach represents an improvement over the manual method and could contribute to improved monitoring and management of these rapidly changing forest environments. This is especially true once user-friendly programs are developed to process the large data sets and the costs of

the CBL decrease. Preliminary results from *Distichlis spicata* dominated marshes suggest that vegetation density is too high to allow ground surface detection. We are currently testing this method in *Spartina patens* and *S. alterniflora* marshes on the US east coast.

### Submergence Potential of Mangroves

To better understand the submergence potential of the mangrove plots that were measured for this study, a wetland sea-level rise rate ( $RSLR_{wet}$ ) was calculated (Cahoon 2015).  $RSLR_{wet}$  is the difference between the tide gage RSLR and the mangrove accretion or SEC rate, which estimates the direction and magnitude of the sea-level trend relative to the mangrove forest floor. Negative or zero  $RSLR_{wet}$  values indicate an elevation surplus and a mangrove that is keeping up with or pacing RSLR. Positive  $RSLR_{wet}$  values indicate an elevation deficit and a mangrove that is not keeping up with RSLR. Lead-210 and SET  $RSLR_{wet}$  rates indicate that only a few of the sites measured (four and five,

**Table 4** Wetland relative sea-level rise (RSLR<sub>wet</sub>) rate determined from <sup>210</sup>Pb accretion rates and SET and CBL SEC rates

Plot	RSLR <sub>wet</sub> ( <sup>210</sup> Pb)	RSLR <sub>wet</sub> (SET)	RSLR <sub>wet</sub> (SET*)	RSLR <sub>wet</sub> (CBL)
ENI INT A	<b>-0.12</b>	1.46	-	-
ENI INT B	3.24	1.52	-	-
ENI INT C	2.02	2.02	-	-
ENI RIV A	2.20	2.17	-	-
ENI RIV B	2.25	2.26	-	-
ENI RIV C	0.64	2.39	10.67	9.75
ENI FRN A	1.16	<b>-0.60</b>	-	-
ENI FRN B	0.27	0.01	-	-
ENI FRN C	0.18	0.75	-	-
SAP INT A	1.75	<b>-1.02</b>	<b>-2.26</b>	<b>-1.84</b>
SAP INT B	1.51	<b>-0.49</b>	<b>-0.97</b>	<b>-3.53</b>
SAP INT C	<b>-2.86</b>	<b>-1.80</b>	-	-
SAP RIV A	2.39	4.49	5.37	1.07
SAP RIV B	1.43	0.78	4.89	4.65
SAP RIV C	<b>-1.29</b>	<b>-1.00</b>	6.85	9.04
SAP FRN B	1.24	2.84	0.78	0.39
SAP FRN C	<b>-0.12</b>	1.46	5.19	6.2

Bold values represent an elevation surplus and a study site that is keeping up with or pacing RSLR

\*SET SEC rates determined over the 2017–2019 time period

respectively) are currently keeping up with RSLR (Table 4). These sites were not the same. Only two of the eight sites where RSLR<sub>wet</sub> was determined from SETs and CBL were keeping up with RSLR and these were the same sites. The discrepancy between <sup>210</sup>Pb and SET sites is due to <sup>210</sup>Pb cores being collected from areas adjacent to the SETs as accretion and SEC rates can vary significantly within the same wetland (Breithaupt et al. 2012; Krauss et al. 2010; MacKenzie et al. 2016). While <sup>210</sup>Pb, SETs, and CBL all appear to be proven methods to monitor the vulnerability of coastal areas to SLR, the number of samples required to effectively capture the spatial variability of accretion or SEC rates is much greater than what has generally been used in previous studies, including this one. More cores and SETs could help to improve our ability to predict mangrove vulnerability or resilience to SLR.

## Conclusion

Of the three methods tested, the traditional SET/rSET method appears to be the most cost-effective method to track changes in forest floor elevation (Table 1). Despite the fact that SETs/rSETs can only track mangrove response to SLR at the annual to decadal scale, this time scale may be more appropriate to examine the relationship among vertical accretion, elevation, and sea-level rise compared to the longer time periods <sup>210</sup>Pb samples (Cahoon and Lynch 1997). The SET/rSET also has the capability of including subsurface processes when they occur, especially when paired with marker horizons (Cahoon and Lynch 1997), though this was not the case in this or other

studies described above. Compared to SETs/rSETs, <sup>210</sup>Pb can be costly to process, in terms of funding, human resources, and time. Lead-210 can yield important information about previous sediment events or previous responses of mangroves to changes in SLR (MacKenzie et al. [in review](#); Rogers et al. 2014; Smoak et al. 2013). If surface root zone processes are more important than subsurface processes in influencing mangrove SEC, then <sup>210</sup>Pb accretion rates can be used to track the vulnerability of mangroves to SLR. The third method, CBL, was the most accurate and precise method to track changes in forest floor elevations but also relies on the SET protocol. However, the CBL method is currently much more expensive than SETs or <sup>210</sup>Pb and results in large data sets that need to be processed. CBL is promising for its ease and efficiency, and as costs come down and accessibility increases, this method may be considered for incorporation into mangrove monitoring programs. Until then, making both SET and CBL measurements should be made together wherever possible can help to increase confidence that both methods are capturing similar changes in surface elevation of mangrove forests.

**Acknowledgements** We thank Ethan Hughes and Emos Eperiam for assistance in data collection. This work was funded by an internal grant from the USDA US Forest Service Pacific Southwest Research Station (“A new tool to monitor the resilience of mangroves to sea-level rise”) as well as grants from the US Fish and Wildlife Service (“Increasing Resilience of Micronesia’s Mangroves”), Department of the Interior U.S. Geological Survey (USGS) Pacific Island Climate Adaptation Science Center (PICASC, “Understanding the future resiliency of mangrove forests to sea-level rise in the Western Pacific: initiating a national assessment approach” G19PG00095), and the USGS Climate R&D Program. Any use of trade, firm, or product name is for descriptive purposes only and does not imply endorsement by the US Government.

**Data Availability** Data is available upon request from the authors.

## Declarations

**Peer Review Disclaimer** This draft manuscript is distributed solely for purposes of scientific peer review. Its content is deliberative and predecisional, so it must not be disclosed or released by reviewers. Because the manuscript has not yet been approved for publication by the US Geological Survey (USGS), it does not represent any official USGS finding or policy.

**Open Access** This article is licensed under a Creative Commons Attribution 4.0 International License, which permits use, sharing, adaptation, distribution and reproduction in any medium or format, as long as you give appropriate credit to the original author(s) and the source, provide a link to the Creative Commons licence, and indicate if changes were made. The images or other third party material in this article are included in the article's Creative Commons licence, unless indicated otherwise in a credit line to the material. If material is not included in the article's Creative Commons licence and your intended use is not permitted by statutory regulation or exceeds the permitted use, you will need to obtain permission directly from the copyright holder. To view a copy of this licence, visit <http://creativecommons.org/licenses/by/4.0/>.

## References

- Alongi, D.M. 2008. Mangrove forests: Resilience, protection from tsunamis, and responses to global climate change. *Estuarine, Coastal and Shelf Science* 76: 1–13.
- Appleby, P., and F. Oldfield. 1978. The calculation of lead-210 dates assuming a constant rate of supply of unsupported  $^{210}\text{Pb}$  to the sediment. *CATENA* 5: 1–8.
- Besl, P.J., and N.D. McKay. 1992. Method for registration of 3-D shapes. In *Sensor fusion IV: Control paradigms and data structures*, 586–606. Spie.
- Bland, J.M., and D. Altman. 1986. Statistical methods for assessing agreement between two methods of clinical measurement. *The Lancet* 327: 307–310.
- Bland, J.M., and D.G. Altman. 1999. Measuring agreement in method comparison studies. *Statistical Methods in Medical Research* 8: 135–160.
- Breithaupt, J.L., J.M. Smoak, R.H. Byrne, M.N. Waters, R.P. Moyer, and C.J. Sanders. 2018. Avoiding timescale bias in assessments of coastal wetland vertical change. *Limnology and Oceanography* 63: S477–S495.
- Breithaupt, J.L., J.M. Smoak, T.J. Smith III, C.J. Sanders, and A. Hoare. 2012. Organic carbon burial rates in mangrove sediments: Strengthening the global budget. *Global Biogeochemical Cycles* 26.
- Brooks, M.E., K. Kristensen, K.J. Van Benthem, A. Magnusson, C.W. Berg, A. Nielsen, H.J. Skaug, M. Machler, and B.M. Bolker. 2017. glmmTMB balances speed and flexibility among packages for zero-inflated generalized linear mixed modeling. *The R Journal* 9: 378–400.
- Cahoon, D.R. 2015. Estimating relative sea-level rise and submergence potential at a coastal wetland. *Estuaries and Coasts* 38: 1077–1084.
- Cahoon, D.R., and J.C. Lynch. 1997. Vertical accretion and shallow subsidence in a mangrove forest of southwestern Florida, USA. *Mangroves and Salt Marshes* 1: 173–186.
- Cahoon, D.R., J.C. Lynch, B.C. Perez, B. Segura, R.D. Holland, C. Stelly, G. Stephenson, and P. Hensel. 2002. High-precision measurements of wetland sediment elevation: II. The rod surface elevation table. *Journal of Sedimentary Research* 72: 734–739.
- Caldwell, A.R. 2022. SimplyAgree: An R package and jamovi module for simplifying agreement and reliability analyses. *Journal of Open Source Software* 7: 4148.
- Callaway, J.C., D.R. Cahoon, and J.C. Lynch. 2013. The surface elevation table–marker horizon method for measuring wetland accretion and elevation dynamics. *Methods in Biogeochemistry of Wetlands* 10: 901–917.
- Dewez, T.J., D. Girardeau-Montaut, C. Allanic, and J. Rohmer. 2016. FACETS: A Cloudcompare Plugin to extract geological planes from unstructured 3D point clouds. *International Archives of the Photogrammetry, Remote Sensing & Spatial Information Sciences* 41.
- Duke, N. 1999. The 1998 survey of *Rhizophora* species in Micronesia. In *Final report to the USDA Forest Service PSW-98-021-RJVA*, 13 pages. Albany, CA.
- Fafard, A., A.R. Kargar, and J. van Aardt. 2020. Weighted spherical sampling of point clouds for forested scenes. *Photogrammetric Engineering & Remote Sensing* 86: 619–625.
- Holgate, S.J., A. Matthews, P.L. Woodworth, L.J. Rickards, M.E. Tamisiea, E. Bradshaw, P.R. Foden, K.M. Gordon, S. Jevrejeva, and J. Pugh. 2013. New data systems and products at the permanent service for mean sea level. *Journal of Coastal Research* 29: 493–504.
- Kargar, A.R., R.A. MacKenzie, M. Apwong, E. Hughes, and J. van Aardt. 2020. Stem and root assessment in mangrove forests using a low-cost, rapid-scan terrestrial laser scanner. *Wetlands Ecology and Management* 28: 883–900.
- Kauffman, J.B., V.B. Arifanti, H.H. Trejo, M.C.J. García, J. Norfolk, M. Cifuentes, D. Hadriyanto, and D. Murdiyarso. 2017. The jumbo carbon footprint of a shrimp: Carbon losses from mangrove deforestation. *Frontiers in Ecology and the Environment* 15: 183–188.
- Krauss, K.W., D.R. Cahoon, J.A. Allen, K.C. Ewel, J.C. Lynch, and N. Cormier. 2010. Surface elevation change and susceptibility of different mangrove zones to sea-level rise on Pacific high islands of Micronesia. *Ecosystems* 13: 129–143.
- Krauss, K.W., K.L. McKee, C.E. Lovelock, D.R. Cahoon, N. Saintilan, R. Reef, and L. Chen. 2014. How mangrove forests adjust to rising sea level. *New Phytologist* 202: 19–34.
- Lander, M.A., and S. Khosrowpanah. 2004. *Rainfall Climatology for Pohnpei Island the Federated States of Micronesia*: Water and Environmental Research Institute of the Western Pacific, University of Guam.
- Lovelock, C.E., M.F. Adame, V. Bennion, M. Hayes, R. Reef, N. Santini, and D.R. Cahoon. 2015a. Sea level and turbidity controls on mangrove soil surface elevation change. *Estuarine, Coastal and Shelf Science* 153: 1–9.
- Lovelock, C.E., D.R. Cahoon, D.A. Friess, G.R. Guntenspergen, K.W. Krauss, R. Reef, K. Rogers, M.L. Saunders, F. Sidik, A. Swales, N. Saintilan, L.X. Thuyen, and T. Triet. 2015b. The vulnerability of Indo-Pacific mangrove forests to sea-level rise. *Nature* 526: 559–562.
- MacKenzie, R.A., M. Apwong, K. Buffington, E. Eperiam, K. Thorne, K.W. Krauss, R. Marquez, T. Greenstone Alefaio, J. Grow, and J.V. Klump. In review. Interisland variability in mangrove resilience to sea level rise Biotic and Abiotic Drivers of resilience to sea-level rise in Pacific high island mangrove forests. *Estuaries and Coasts*.
- MacKenzie, R.A., P.B. Foulk, J.V. Klump, K. Weckerly, J. Purbospito, D. Murdiyarso, D.C. Donato, and V.N. Nam. 2016. Sedimentation and belowground carbon accumulation rates in mangrove forests that differ in diversity and land use: A tale of two mangroves. *Wetlands Ecology and Management* 24: 245–261.
- McKee, K.L., D.R. Cahoon, and I.C. Feller. 2007. Caribbean mangroves adjust to rising sea level through biotic controls on

- change in soil elevation. *Global Ecology and Biogeography* 16: 545–556.
- Osland, M.J., A.C. Spivak, J.A. Nestlerode, J.M. Lessmann, A.E. Almario, P.T. Heitmuller, M.J. Russell, K.W. Krauss, F. Alvarez, and D.D. Dantin. 2012. Ecosystem development after mangrove wetland creation: Plant–soil change across a 20-year chronosequence. *Ecosystems* 15: 848–866.
- Parkinson, R.W., C. Craft, R.D. DeLaune, J.F. Donoghue, M. Kearney, J.F. Meeder, J. Morris, and R.E. Turner. 2017. Marsh vulnerability to sea-level rise. *Nature Climate Change* 7: 756–756.
- PSMFS. 2023. Tide gauge data, Retrieved 19 Jun 2020 from <http://www.psmfsl.org/data/obtaining/>.
- R Core Team, R. 2013. R: A language and environment for statistical computing.
- Ranjan, R.K., J. Routh, A.L. Ramanathan, and J.V. Klump. 2011. Elemental and stable isotope records of organic matter input and its fate in the Pichavaram mangrove–estuarine sediments (Tamil Nadu, India). *Marine Chemistry* 126: 163–172.
- Robbins, J.A. 1978. Geochemical and geophysical application of radioactive lead. In *The biogeochemistry of lead in the environment*, ed. J.O. Nriagu. Amsterdam: Elsevier/North-Holland Biomedical Press.
- Robbins, J.A., D.N. Edgington, and A.L.W. Kemp. 1975. Comparative  $^{210}\text{Pb}$ ,  $^{137}\text{Cs}$ , and pollen geochronologies of sediments from Lakes Ontario and Erie. *Quaternary Research* 10: 256–278.
- Robbins, J.A., and D.N. Edgington. 1975. Determination of recent sedimentation rates in Lake Michigan using Pb-210 and Cs-137. *Geochimica Et Cosmochimica Acta* 39: 285–304.
- Rogers, K., J.J. Kelleway, N. Saintilan, J.P. Megonigal, J.B. Adams, J.R. Holmquist, M. Lu, L. Schile-Beers, A. Zawadzki, and D. Mazumder. 2019. Wetland carbon storage controlled by millennial-scale variation in relative sea-level rise. *Nature* 567: 91–95.
- Rogers, K., N. Saintilan, and C.D. Woodroffe. 2014. Surface elevation change and vegetation distribution dynamics in a subtropical coastal wetland: Implications for coastal wetland response to climate change. *Estuarine, Coastal and Shelf Science* 149: 46–56.
- Rouzbeh Kargar, A., R.A. MacKenzie, A. Fafard, K.W. Krauss, and J. van Aardt. 2020. Surface elevation change evaluation in mangrove forests using a low-cost, rapid-scan terrestrial laser scanner. *Limnology and Oceanography: Methods*.
- Rusu, R.B., Z.C. Marton, N. Blodow, M. Dolha, and M. Beetz. 2008. Towards 3D point cloud based object maps for household environments. *Robotics and Autonomous Systems* 56: 927–941.
- Saintilan, N., N. Khan, E. Ashe, J. Kelleway, K. Rogers, C.D. Woodroffe, and B. Horton. 2020. Thresholds of mangrove survival under rapid sea level rise. *Science* 368: 1118–1121.
- Sharma, S., R.A. MacKenzie, T. Tieng, K. Soben, N. Tulyasuwan, A. Resanond, G. Blate, and C.M. Litton. 2020. The impacts of degradation, deforestation and restoration on mangrove ecosystem carbon stocks across Cambodia. *Science of the Total Environment* 706: 135416.
- Smoak, J.M., J.L. Breithaupt, T.J. Smith III., and C.J. Sanders. 2013. Sediment accretion and organic carbon burial relative to sea-level rise and storm events in two mangrove forests in Everglades National Park. *CATENA* 104: 58–66.
- Swales, A., S.J. Bentley Sr., and C.E. Lovelock. 2015. Mangrove-forest evolution in a sediment-rich estuarine system: Opportunists or agents of geomorphic change? *Earth Surface Processes and Landforms* 40: 1672–1687.
- Swales, A., and C.E. Lovelock. 2020. Comparison of sediment-plate methods to measure accretion rates in an estuarine mangrove forest (New Zealand). *Estuarine, Coastal and Shelf Science* 236: 106642.
- Trochu, F. 1993. A contouring program based on dual kriging interpolation. *Engineering with Computers* 9: 160–177.
- Webb, E.L., D.A. Friess, K.W. Krauss, D.R. Cahoon, G.R. Guntenspergen, and J. Phelps. 2013. A global standard for monitoring coastal wetland vulnerability to accelerated sea-level rise. *Nature Climate Change* 3: 458–465.
- Whelan, K.R., T.J. Smith, G.H. Anderson, and M.L. Ouellette. 2009. Hurricane Wilma's impact on overall soil elevation and zones within the soil profile in a mangrove forest. *Wetlands* 29: 16–23.
- Woltz, V.L., E.I. Peneva-Reed, Z. Zhu, E.L. Bullock, R.A. MacKenzie, M. Apwong, K.W. Krauss, and D.B. Gesch. 2022. A comprehensive assessment of mangrove species and carbon stock on Pohnpei. *Micronesia. Plos One* 17: e0271589.
- Woodroffe, C.D., C.E. Lovelock, and K. Rogers. 2015. Mangrove shorelines. *Coastal environments and global change* 251–267.
- Zai, D., J. Li, Y. Guo, M. Cheng, P. Huang, X. Cao, and C. Wang. 2017. Pairwise registration of TLS point clouds using covariance descriptors and a non-cooperative game. *ISPRS Journal of Photogrammetry and Remote Sensing* 134: 15–29.
- Zhang, W., J. Qi, P. Wan, H. Wang, D. Xie, X. Wang, and G. Yan. 2016. An easy-to-use airborne LiDAR data filtering method based on cloth simulation. *Remote Sensing* 8: 501.
- Zlot, R., and M. Bosse. 2009. Place recognition using keypoint similarities in 2D LiDAR maps. In *Experimental Robotics: The Eleventh International Symposium*, 363–372: Springer.